A Slotted Test Section Numerical Model for Interference Assessment

William B. Kemp Jr.*
The College of William and Mary, Williamsburg, Virginia

A numerical model of a slotted wind tunnel test section, intended for use with sparsely measured wall pressures in a wall interference assessment procedure, is described. The numerical model includes a discrete, finite-length wall slot representation and accounts for the nonlinear effects of the dynamic pressure of the slot outflow jet and of the low energy of slot inflow air. By using the numerical model in a wall interference prediction mode, it is demonstrated that accounting for slot discreteness is important in interpreting wall pressures measured between slots, and that accounting for finite slot length and nonlinear effects in the slot boundary condition can yield significant departures from the wall interference predicted using the classical linear homogeneous infinite-length wall representation.

Nomenclature

a = slot width
C = cross section area of test section
C_D = drag coefficient
C_L = lift coefficient
d = slot spacing
h = tunnel half height
K = dimensionless coefficient in equivalent homogeneous slotted wall boundary condition
$\tilde{K}$ = coefficient in discrete slot boundary condition
$\Delta K'$ = increment in K due to distance from slot
P = slotted wall parameter, $1/(1+Kd/h)$
R = coefficient in porous wall boundary condition
r = radius of slot inflow bubble
S = line source strength, also test model reference area
u,v,w = velocity perturbations in x, y, and z directions, respectively, normalized by tunnel reference velocity
V = test model volume
x,y,z = Cartesian coordinates
Δ = increment
δ = lift interference parameter at model location, $w_{LI}C/SC_L$
ϵ = slot control point recession distance
σ = panel source sheet strength
ϕ = perturbation potential
$\tilde{\phi}$ = perturbation potential outside the boundary of tunnel flow domain

Subscripts

d = pertaining to slot discretizing perturbation
h = pertaining to equivalent homogenous slotted wall
LI = lift interference
n = normal to wall
p = plenum chamber condition
r = condition at distance r from line source
SB = solid blockage
WB = wake blockage
0 = condition at slot origin
ϵ = condition at distance ϵ from line source

Introduction

IN recent years, a significant effort has been directed to the development of methods that make use of measured wall pressures in the assessment of and correction for wall interference in wind tunnel tests. These methods offer an attractive alternative to the adaptive wall techniques as a means of minimizing the testing errors due to wall interference. Such methods are particularly important for transonic tunnels because the classical interference prediction methods have been found inadequate for slotted or perforated test sections.

The development of wall interference assessment and correction methods for application to two-dimensional airfoil tests has reached a relatively mature state.[1,2] The excellent survey of Ref. 3 clarifies the role of such methods within the broad scope of theoretical approaches to the problem of two-dimensional wind tunnel wall interference. For three-dimensional applications, however, satisfactory interference assessment methods are not yet available. One reason is that an inordinate amount of experimental data is required to define the boundary data surfaces needed for three-dimensional assessment computations. Mokry[4] simplified this problem by representing the test model as a point disturbance and using an azimuthal harmonic description of the outer boundary. Wall pressures measured in four longitudinal rows were used to define the lowest order harmonics, and higher harmonics were ignored. Rizk et al.[5,6] used a more realistic representation of the test model based on the known model geometry and measured forces and moments but assumed that the measured data available were sufficient to define fully an outer computational boundary near the tunnel walls.

The results to be described in this paper were obtained in a study undertaken to develop a new outer boundary treatment having wall data requirements comparable to the Mokry method while yielding an outer boundary description with accuracy closely approaching that assumed in the methods of Rizk et al. In concept, the outer computational boundary is provided by a numerical model of the tunnel test section capable of representing geometric details having a small size relative to the characteristic tunnel dimensions, and formulated in terms of boundary condition parameters that can be controlled to reproduce the pressure distributions measured along several longitudinal rows in the tunnel. For this purpose the numerical model should provide a realistic representation of all test section features capable of affecting significantly the pressure at the measurement locations. The numerical model described herein was developed in an attempt to satisfy this requirement. It is applicable to test sections having open (unbaffled) wall slots and is limited at present to subcritical wall flows. In keeping with the practice developed for two-dimensional interference assessment, viscosity effects at the wall are not modeled overtly but are assumed to be accounted for by adjusting the parameters of inviscid form boundary conditons to match measured

Presented as Paper 84-0627 at the AIAA 13th Aerodynamic Testing Conference, San Diego, Calif., March 5-7, 1984; received May 21, 1984; revision received Oct. 26, 1984.

*Senior Research Associate. Associate Fellow AIAA.

pressures. Confidence in the validity of this approach is strengthened by the results of Sedin and Sorensen,[7] which show that, for the axisymmetric case studied, adjustment of such parameters in a theoretical inviscid slot boundary condition yielded good agreement with measured model pressures at the tunnel centerline.

The model is a system of linear equations largely based on high order panel method technology as implemented by Thomas.[8] A computationally efficient algorithm is used for iterative update of the solution if certain nonlinear features are included. A discrete slot representation is used; thus the model is appropriate for matching pressures measured on the solid wall segments between slots. This feature should eliminate the need for introducing such intrusive devices as rails or pipes to provide pressure instrumentation.

Although the procedure for matching measured pressures is not finalized at the time of this writing, the test section model can be used as an interference prediction tool by specifying all boundary conditions without regard to measured pressures. Results from such use are presented herein to illustrate the significance of several slotted tunnel features that are deemed important for the intended use of the model in an assessment procedure but have been documented only to a limited extent in the literature. These features include discrete slot effects, the effects of finite slot length coupled with the flow quantity constraint imposed by the plenum, and the nonlinear effects arising from the dynamic pressure in the outflow jets issuing from the slots into the plenum and from the low energy of inflow air from the plenum. All of these features are recognized in the computational method based on the theory developed by Berndt[9] and applied at transonic speeds by Sedin and Sorensen[7] in a form limited to nonlifting axisymmetric flows. Earlier studies of some of these features include that by Steinle and Pejack[10] using the WALINT program, which predicts the lift interference in a tunnel with discrete porous slots of infinite length, the studies by Lo and Glassman[11] and by Sloof and Piers[12] of finite length effects for perforated walls, and the inclusion by Wood[13] of nonlinear slot cross-flow effects in a two-dimensional blockage interference solution. The capability of the present numerical model to represent other features, including a general test model, sting and sting support, wall divergence and shaping, and slot flow re-entry flaps is noted.

Description of Numerical Model

Basic Linear Form

The basic elements used for modeling the flow in a slotted wind tunnel test section are illustrated in Fig. 1. Only one half the tunnel is modeled; the other half is represented by symmetry considerations. The solution domain is the interior of a rectangular parallelepiped. Source and doublet singularities are distributed over the boundaries of this domain such that the flow exterior to the solution domain can be considered (in a limited sense) to be unperturbed. Thus, the perturbation potential and normal velocity of the interior flow at the boundaries are approximately equal to the local doublet and source strength, respectively. The singularity distributions are discretized into panels within which the source strength is either constant or bilinear and the doublet strength is either constant or biquadratic. The panels on any boundary representing the top, side, or bottom tunnel wall are grouped into one or more networks. Continuity of the higher order singularity strength across panel boundaries within a network is enforced in a least square sense. The basic boundary condition of zero perturbation potential in the exterior flow ($\bar{\phi}=0$) is imposed at control points located at the panel centers. The biquadratic networks have additional control points located along the network edges at which either the basic or special boundary conditions are imposed.

A general purpose panel method program developed by Thomas,[8] which includes the higher order paneling capabilities noted above, was used as a starting point for the present numerical model. Certain wind tunnel features have been added in the form of singularities whose strengths can be specified a priori. These include wall divergence and the sting support sector, modeled by source panels, the sting, modeled as a slender body, and the test model which can be represented either as a point disturbance or a distributed system of volume and lift of the form used by Rizk and Smithmeyer.[5]

The slotted wall regions of the tunnel can be represented either as a homogeneous wall or with discrete slots. Consider first the homogeneous case. The linearized homogeneous slotted wall boundary condition may be written

$$u-u_p+Kd\frac{\partial v_n}{\partial x}=0 \tag{1}$$

This wall is modeled by superimposing a network of bilinear source panels over the doublet panels in the slotted wall region and imposing at the panel centers a boundary condition obtained by integrating Eq. (1)

$$\phi-\phi_0+Kd\,v_n=u_p(x-x_0) \tag{2}$$

Because the basic $\bar{\phi}=0$ condition is also imposed at these points, both the source and doublet panel strengths are treated as unknowns to be determined during the solution. The local homogeneous normal velocity is then given by $v_n=-\sigma_h$.

The model of the discretely slotted wall is developed using the homogeneous wall as a starting point, and superposing additional singularities to collect the wall flux into discrete lines. The discretizing perturbation is generated by the combination of a source sheet of strength

$$\sigma_d=2v_n \tag{3}$$

to cancel the smoothly distributed wall flux in the interior flow and a set of source (or sink) lines at the slot locations of strength

$$S=-\int_{-d/2}^{d/2}\sigma_d\,dy \tag{4}$$

to replace the distributed wall flux with a concentrated flux of the same magnitude. Equation (4) also ensures that the discretizing singularity model introduces no net source strength from any element extending half the slot spacing to each side of a slot. The discretizing perturbation, therefore, should die out rapidly with distance away from the wall.

To implement this concept in the numerical model, the line sources as well as the longitudinal edges of the source and doublet panels are placed at the slot locations. The line source strength S is quantified at the panel corners, varies linearly on the intervening segments, and has a value of zero at the upstream and downstream ends of each slot. The panel source strength is obtained by combining the homogeneous wall and discretizing sheet strengths, and its value at each panel edge

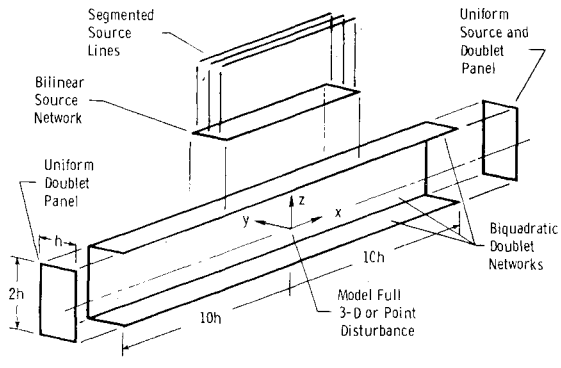

Fig. 1 Elements used in numerical model of slotted test section.

midpoint adjacent to a slot is linked to the local value of S to assure that Eq. (4) is satisfied.

The relations given previously may be combined to specify the total source sheet strength σ in terms of S as

$$\sigma = \sigma_h + \sigma_d = \tfrac{1}{2}\sigma_d = -(S/2d) \tag{5}$$

Using Eq. (2), (3), and (5), the discrete slot boundary condition is written

$$\phi - \phi_0 - \tfrac{1}{2}\tilde{K}S = u_p(x - x_0) \tag{6}$$

which is enforced as a boundary condition at control points near the slots. The influence of the slot discretizing perturbation is omitted from the basic $\tilde{\phi} = 0$ condition which is imposed at all panel center control points, including those on the slotted wall. The slot control points are recessed a small distance ϵ into the interior flow from the line sources representing the slots. This recession distance can be related approximately to the slot width by assuming that the radial velocity across a semicircle of radius ϵ centered on the line source should be equal to the transverse velocity through a slot of width a in the wall being modeled. Accordingly,

$$\epsilon = a/\pi \tag{7}$$

The panel doublet strengths and line source strengths are both treated as unknowns constrained by boundary conditions at the panel centers and slot control points.

Linear Discrete Slot Validation

To examine some properties of this discrete slot representation, the numerical model was used to solve the flow in a long duct with full length discrete slots on the top wall and an upward transpiration introduced over the entire bottom wall by means of a uniform strength source sheet. The solution showed that at a sufficient distance from the upstream end, an equilibrium condition was reached in which the flux absorbed by the line sinks on the top wall just matched that introduced uniformly over the bottom wall and all longitudinal velocity gradients vanished. The equilibrium level of the longitudinal perturbation velocity was set to zero by an appropriate choice of the velocity entering the upstream end of the duct. The resulting flow in the equilibrium region is a two-dimensional flow in the duct cross-section planes.

From this solution, the potential distributions along two vertical lines were determined and are shown in a normalized form in Fig. 2. The distribution labeled $y = 0$ is aligned with one of the top wall slots and shows the increasing vertical gradient of potential as the sink line is approached. The distribution at $y = \pm 0.5d$ shows the potential gradient vanishing at the stagnation point halfway between slots. At a distance from the wall of less than one slot spacing the two distributions have become essentially coincident with a gradient of unity. The distribution corresponding to an equivalent homogeneous wall representation is obtained by extrapolating this interior flow to the wall with a constant gradient. The homogeneous slot parameter K is found, by rearranging Eq. (2), to represent the jump in potential (normalized relative to $v_n d$) between the boundary value in the tunnel flow and a reference value in the plenum, and is so indicated on Fig. 2.

For the discrete slot representation, the normalized potential curve at $y = \pm 0.5d$ reaches the wall with a vanishing normal gradient, indicating stagnation of the transverse flow halfway between slots. The potential value at this point differed from the homogeneous wall boundary value by about 0.22, which agrees with the incremental value derived by Berndt and Sorensen.[14]

The normalized potential curve labeled $y = 0$ on Fig. 2 can be interpreted as the locus of combinations of ϵ and $\tilde{K}$ required to produce the same flow in the tunnel far from the wall as the homogeneous wall model, if K and $\tilde{K}$ are measured from the same plenum reference value. It is clear that with the discrete slot model, the acceleration of tunnel interior flow toward the slot provides, in the solution, some of the potential growth that must be supplied entirely by the boundary condition in the homogeneous wall model. This discretization increment in normalized potential is shown in Fig. 3 as a function of slot openness ratio a/d by using the simple assumption of Eq. (7) to relate a to ϵ. Figure 3 shows that this variation is a close approximation of the classical log cosecant form of the homogeneous wall slot parameter K as given by Davis and Moore.[15] It was determined empirically that the assumption of

$$d/\epsilon = 4.08(d/a) - 3.0 \tag{8}$$

instead of Eq. (7) would produce almost exact agreement between the curves on Fig. 3. By using this empiricism to relate the control point recession ϵ to an equivalent slot width a, the discrete slot boundary condition in the present numerical model can be related algebraically to the more familiar homogeneous slotted wall boundary condition producing the same tunnel interior flow far from the slots by

$$K = \tilde{K} + \frac{1}{\pi}\ell n \csc\left(\frac{\pi}{2}\frac{a}{d}\right) \tag{9}$$

Equations (8) and (9) show that the simulated slot width ratio a/d for discrete slots may be changed by varying either the boundary condition parameter $\tilde{K}$ or the control point recession ϵ. The equivalence of this simulation to the homogeneous wall representation was checked for the case of a point lift disturbance in a tunnel of infinite length having a square cross section with solid side walls and six slots in each of the top and bottom walls. The results are given in Fig. 4, which shows the lift interference parameter δ at the model location as a function of the slotted wall parameter P of the top and bottom walls. The homogeneous wall case, calculated

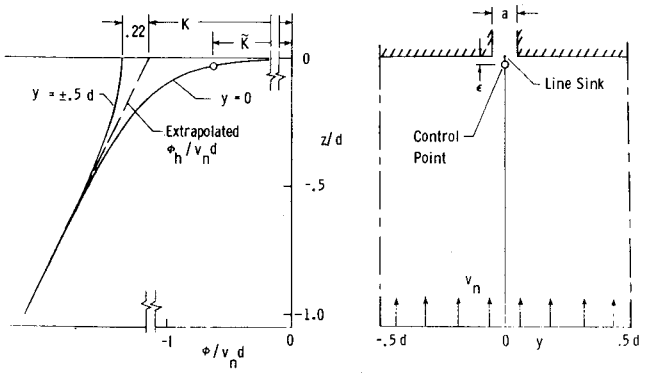

Fig. 2 Characteristics of the discrete slot model in a uniform cross-flow.

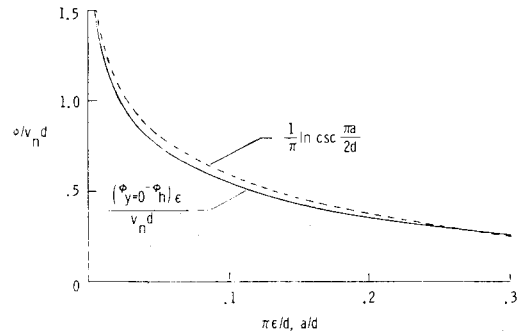

Fig. 3 Comparison of potential growth approaching a discrete slot in uniform cross-flow with homogeneous wall theory.

using the Fourier transform series solution given in Ref. 16 for this tunnel geometry, is shown for comparison. The present method, with ϵ fixed at a small distance and $\tilde{K}$ varying, showed excellent agreement with the homogeneous wall theory over the entire range of P from 0 (solid wall, approximated by $\tilde{K}=10{,}000$) to 1.0 (open wall, requiring $\tilde{K}<0$). With $\tilde{K}=0$ and ϵ varying, excellent agreement was obtained for values of P of 0.5-0.8. For $P>0.9$ (corresponding to $a/d>0.22$), ϵ becomes a significant fraction of the tunnel half height and the flow at the slot control points no longer represents the flow at the wall location. For $P<0.48$ ($a/d<3\times10^{-5}$) the calculated value of δ becomes that for the solid wall because ϵ diminishes into an arbitrarily dimensioned domain where the influence of the adjacent line source is calculated by a limiting form appropriate for $\epsilon=0$.

Results calculated by the WALINT method of Steinle and Pejack[10] are also shown on Fig. 4. In this method, the tunnel walls are built up of infinite length panels. A boundary condition representing either a solid or porous surface is imposed along the centerline of each panel. For the results shown on Fig. 4, each slot was represented by a panel with a width equal to the slot width and a very high porosity coefficient ($R=10{,}000$) in the boundary condition. Fair agreement with the homogeneous wall lift interference was obtained for $P>0.6$ but significant error is apparent for lower values of P. For both discrete slot methods, control of the simulated slot width by controlling a geometric feature of the numerical representation (panel width in the WALINT method and control point recession in the present method) is applicable only in a limited range of slot widths. Control of the simulated slot width through the boundary coefficient $\tilde{K}$ in the present method appears to be free of such limitations.

Nonlinear Slot Model

It has long been recognized that the use of a small perturbation assumption to linearize boundary conditions is particulary restrictive in the case of a slotted tunnel wall because of the slot amplification of transverse velocity by the ratio d/a. As early as 1963, Wood[13] described the formulation of a nonlinear slotted-wall boundary condition and showed numerical results from its application to the solid-blockage case of a nonlifting airfoil in a two-dimensional tunnel. Later, Berndt and Sorensen[14] formulated a nonlinear boundary condition with similar features. This condition has been adapted to account for key viscous effects by Sedin and Sorensen,[7] who demonstrated good agreement with experiment for axisymmetric flows. Two significant nonlinear features are recognized in these formulations. The first feature recognizes that, in the case of slot outflow, part of the pressure difference across a slotted wall should be balanced against the dynamic pressure of the transverse jet issuing from the slot. The second recognizes that, in the case of inflow from the plenum to the tunnel, the behavior of the slot depends on whether the inflowing air is high energy air that originated in the tunnel or low energy air that originated in the plenum. The inflow case is more complex and less well understood than the outflow case.

In the present numerical model, the jet dynamic pressure effect for outflow is represented by a quadratic term in the slot boundary condition. In a form analogous to Eq. (1), the nonlinear homogeneous wall boundary condition could be written

$$u-u_p+Kd\frac{\partial v_n}{\partial x}=\frac{-v_n^2}{2}\left(\frac{d}{a}\right)^2, v_n>0$$

$$=0 \qquad , v_n\le 0 \tag{10}$$

Using the substitution $S=-2dv_n$ leads to the discrete slot form:

$$u-u_p-\frac{1}{2}\tilde{K}\frac{\partial S}{\partial x}=\frac{-S^2}{8a^2}, S<0$$

$$=0 \qquad , S\ge 0 \tag{11}$$

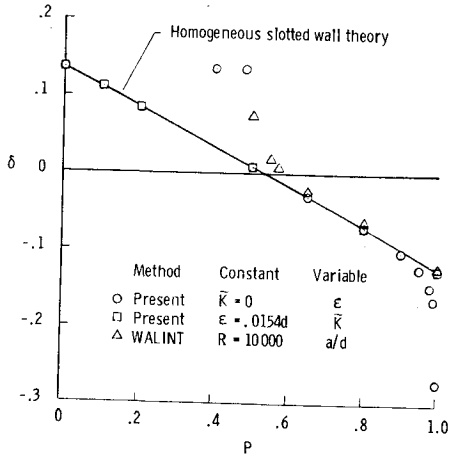

Fig. 4 Comparison of lift interference at model from discrete slot methods with that from homogeneous slotted wall theory, zero span model, square tunnel, six slots in each horizontal wall.

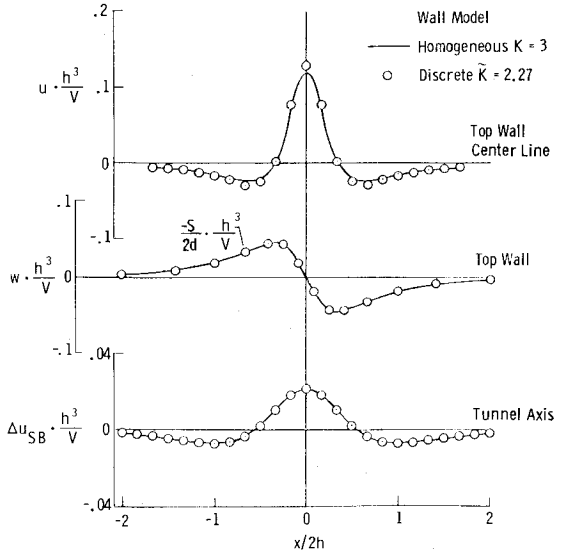

a) Longitudinal distributions.

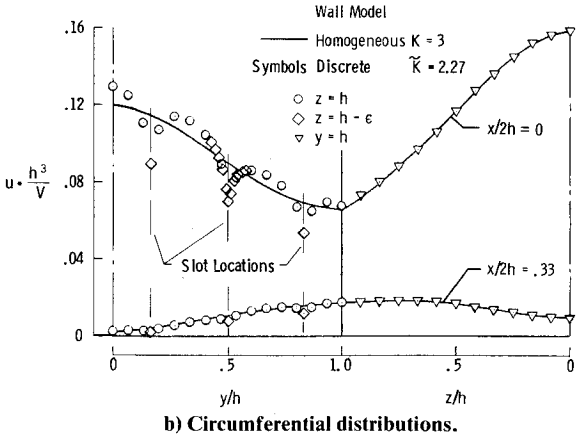

b) Circumferential distributions.

Fig. 5 Effect of discrete slot representation on velocities in infinite length wind tunnel, solid blockage case.

The nonlinear effect of slot inflow is modeled under the assumption that all fluid entering the tunnel through each slot has low velocity and accumulates in a tubular bubble semicircular in cross section and centered on the slot. The cross-sectional area of the bubble is the longitudinal integral of half the line source strength starting at the origin of inflow. Under the assumption that the air in the bubble is essentially quiescent, the plenum pressure should be felt at the boundary of the bubble. Conceptually, the boundary condition on the tunnel flow could be implemented by setting $\tilde{K}=0$ in the slot boundary condition equation (6) and imposing the resulting condition at control points recessed into the tunnel by the radius r of the bubble. The computational work for this procedure would be very large because of the need to recalculate the influence coefficients of all singularities on the relocated control points and solve a new matrix equation at each iteration step.

In the procedure actually used, the slot control points are held at a fixed recession distance ϵ and the $y=0$ curve of Fig. 2 used to determine the value of $\tilde{K}$ at $z=\epsilon$ which would result in $\tilde{K}=0$ at $z=r$. For this purpose, the $y=0$ curve of Fig. 2 is expressed analytically as

$$\Delta K_r' = \frac{r}{d} - \frac{1}{\pi} \ell n \csc\left(\frac{\pi}{2}\frac{a}{d}\right) \tag{12}$$

where a/d is expressed as a function of r/d by use of Eq. (8). The fully nonlinear slot boundary condition now may be written

$$u - u_p - \frac{1}{2}\tilde{K}\frac{\partial S}{\partial x} = \frac{-S^2}{8a^2} \quad ,S<0 \text{ and } r=0$$
$$= \frac{1}{2}\Delta\tilde{K}\frac{\partial S}{\partial x} \quad ,S\geq 0 \text{ or } r>0 \tag{13}$$

where

$$\Delta\tilde{K} = -\tilde{K} + \Delta K_\epsilon' - \Delta K_r' \tag{14}$$

Note that if an outflow region occurs downstream of an inflow region, the outflow is used first to reduce the bubble radius to zero before the outflow dynamic pressure term is invoked. An alternative form of the slot boundary condition is obtained by integrating Eq. (13) along the slot with recognition that S is discretized into linearly varying segments and can change sign within a segment.

To solve the system of equations, the nonlinear terms, which are included in the right-hand side of the system of otherwise linear equations, are ignored in a first trial solution and then evaluated iteratively for subsequent solutions. The Gaussian elimination procedure used to solve the system invokes a triangular factorization of the left-hand side coefficient matrix followed by back substitution of the right-hand side. By saving the factored matrix from the first iteration, the computer time required to solve the nonlinear system of equations, which involved about 120 iterations in the worst cases, was no more than twice that required to solve the linear system alone.

Results

The following sections present results from use of the numerical model to illustrate the effects on slotted test section flows of successively increasing the degree of realism. For all results shown, the tunnel geometry considered is a square cross section with half height h, solid walls, and slotted top and bottom walls with three slots on each side of the centerline. A slot open area ratio $a/d=.06$ was assumed, which is represented according to Barnwell's correlation[17] by $K=3$ in the homogeneous wall boundary condition. The walls were paneled such that four panels were used across the half width

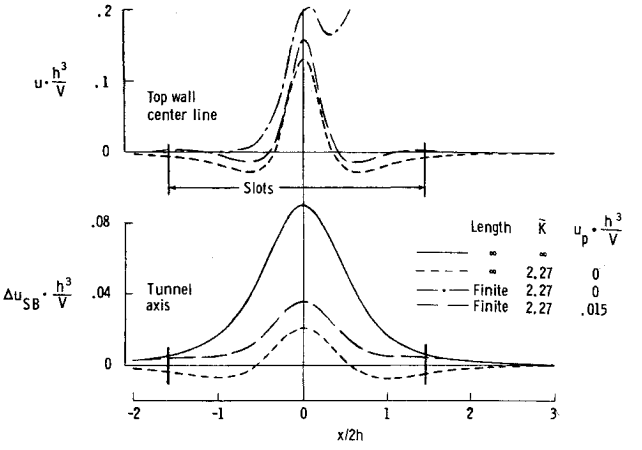

Fig. 6 Effects of finite test section length, solid blockage case.

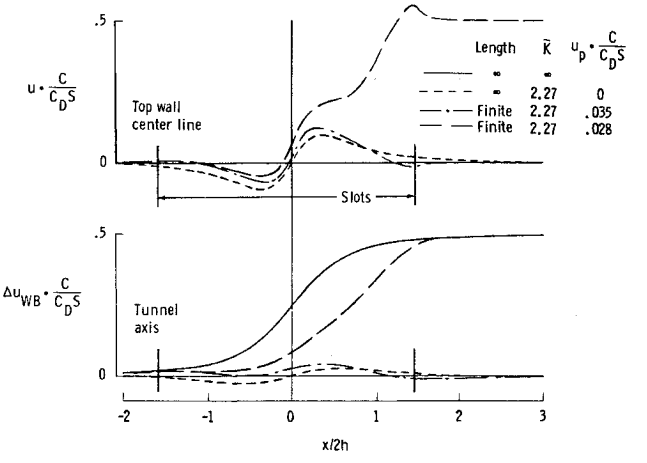

Fig. 7 Effects of finite test section length, wake blockage case.

of the top and bottom walls and six across the height of the side wall. Longitudinally, the computational domain extended $\pm 10h$ from the model location and was divided into either 20 or 21 panel lengths, 12 of which were included in the region representing a finite length test section that extended about $\pm 3h$ from the model. The infinite length test section was approximated by allowing the slots to extend the full $\pm 10h$ length of the paneled region.

In order to facilitate comparison with the existing literature, the test model was represented only as a point doublet, point source, or point lifting system and the sting, sting support sector, and wall shaping features were not used. A Mach number of zero was assumed for all cases.

Discrete Slot Effects

In Fig. 5, discrete slot results, shown by symbols, are compared with results from the homogeneous wall model with identical panel geometry for the case of solid blockage represented by a point doublet in the infinite length test section. All values are normalized by V/h^3. Figure 5a shows the longitudinal distributions of the longitudinal velocity perturbation on the top wall centerline, the vertical (normal) velocity on the top wall centerline (or its discrete slot equivalent, $-S/2d$, at the slot closest to the centerline), and the wall-induced solid blockage velocity on the tunnel axis.

The homogeneous wall results were obtained with $K=3$ for the top and bottom walls. For the discrete slot case, the slot control points were located according to Eq. (7) and a value of $\tilde{K}=2.27$ was used. The wall-induced velocity distributions on

the tunnel axis were found to be in excellent agreement with the homogeneous $K=3$ results, not only for the solid blockage case shown, but also for wake blockage and lift interference. At the top wall, however, discrete slot effects are apparent in the longitudinal velocity even though the equivalent vertical velocity distributions are in excellent agreement. It appears that the discrete slot effect on longitudinal velocity at the wall between slots is approximately proportional to the longitudinal gradient of the normal velocity (or flux through the slots). This result is consistent with the observation relative to Fig. 3 that the normal flow stagnation effect is expressible as an increment in K.

Figure 5b shows the circumferential distribution of longitudinal velocity perturbation along the top wall from the centerline to the tunnel corner and down the side wall to the centerline. Significant effects of slot discreteness are apparent at $x/2h=0$. It is clear that if pressures measured halfway between slots are to be used in an interference assessment procedure, the outer computational boundary should not be formed simply by a smooth interpolation between such pressures. Figure 5b suggests that pressures measured about one sixth of the slot spacing to either side of the slots might be more suitable for such use, so that the smoothly faired surface would approximate more closely the homogeneous wall pressures yielding the same interference at the model. The present discrete slot model should generate an appropriate outer computational boundary, however, when matched to pressures measured at arbitrary locations on the slotted wall.

Effects of Finite Test Section Length

Longitudinal distributions of the longitudinal perturbation velocity on the top wall centerline and of the wall-induced velocity on the tunnel axis are shown in Figs. 6, 7, 8 for point disturbance test models yielding solid blockage, wake blockage, and lift interference respectively. In each figure, results for finite-length slots extending over a range of $x/2h$ values from -1.58 upstream to 1.46 downstream of the model location are compared with results for full-length slots representing the infinite test section length cases. All slotted-wall results were obtained using the discrete slot representation on the top and bottom walls. Wall-induced velocity distributions for the full-length solid-wall test section are included for comparison. It was found that with each type of model disturbance, the magnitude and gradient of the wall-induced velocity at the model location for the solid-wall and infinite length slotted-wall cases are in excellent agreement with predictions developed from Pindzola and Lo[16] using K values of ∞ and 3, respectively.

Consider first the solid blockage results shown on Fig. 6. When the plenum pressure represented by u_p in the slot boundary condition was held at zero, satisfactory results were obtained for the infinite length case. With a finite slot length, however, the need to recognize explicitly the constraint imposed by a sealed or pumped plenum on the total slot flux became apparent. The top wall velocity curve on Fig. 6 for a finite slot length with $u_p=0$ was calculated using an early version of the numerical model and illustrates the problem. The inward flow through the slots downstream of the model far exceeded the outward flow upstream of the model and the additional flow quantity in the duct resulted in velocities downstream of the model which are too high to be plotted in Fig. 6. The unbalanced slot flux was found to be very sensitive to changes in the specified plenum pressure. Consequently, a constraint on total slot flux representing a sealed or pumped plenum chamber was added to the numerical model such that the value of u_p required to satisfy the constraint appears in the solution and is noted in the key for the final curve on Fig. 6. The velocity at the top wall, as well as the wall-induced solid blockage velocity, is shifted upward by about this same amount relative to the infinite length case, resulting in a significant departure from the classical prediction of solid blockage interference.

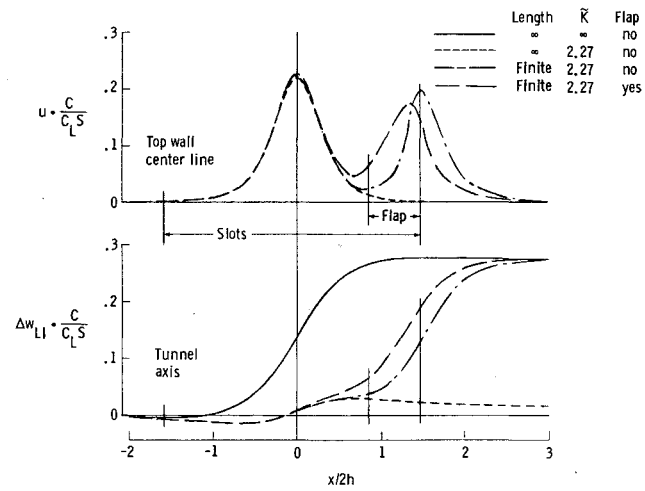

Fig. 8 Effects of finite test section length, lift interference case.

For the wake blockage results shown in Fig. 7, the test model is represented by a point source. The added mass flow either may be bled off through the slots (simulating plenum pumping), causing only minimal finite length effects, or forced to enter the solid wall duct downstream of the slotted section (simulating a sealed plenum), in which case both the magnitude and gradient of the wake blockage interference velocity at the model are shifted significantly toward the solid-wall values.

In the case of lift interference, shown in Fig. 8, the wall-induced velocity on the tunnel axis is directed vertically. With finite-length slots, the wall-induced upwash must become large enough to cancel the downwash induced by the test model and turn the flow back to the direction of the tunnel axis. This turning is associated with a velocity peak at the downstream end of the top wall slots and a corresponding velocity depression on the bottom wall (not shown). Without special treatment, the turning probably is too abrupt to be realistic for those slotted-wall tunnels that utilize a re-entry flap to promote smooth flow at the downstream end of the slots. In such tunnels, the pressure in the confined region between a slot and its re-entry flap must depart from the plenum pressure in such a way that the slot flux is reduced smoothly to zero at the slot end.

To simulate such a re-entry flap in the numerical model, the slot boundary condition is altered for those control points lying between the flap leading edge and the slot end to include an increment in u_p that varies linearly from zero at the flap leading edge to an unknown value Δu_p at each slot end while the value of S at each slot end is set to zero. This flap simulation was included in the finite length results given in Figs. 6 and 7. The effect on lift interference (as shown on Fig. 8) of including such a flap is to cause the downstream slot end effects to be felt somewhat farther upstream. For the tunnel geometry considered herein, the magnitude and gradient of the wall-induced upwash at the model center are not affected by the finite slot length, although some effect is observed just downstream of the model center where a tail might be located.

Effects of Nonlinear Slot Boundary Condition

Distributions on the tunnel axis of wall-induced velocities resulting from the nonlinear slot boundary conditions are compared in Fig. 9 with those previously shown for the linear boundary condition. The slot boundary condition given by Eq. (11) was used to include the nonlinear effects of only the slot outflow dynamic pressure, while Eq. (13) was used for the combined outflow and inflow nonlinearities. Values of the model disturbance strengths were selected to represent a model size somewhat larger than that usually tested in a slotted test section. The strengths used are $V/h^3=.025$ for

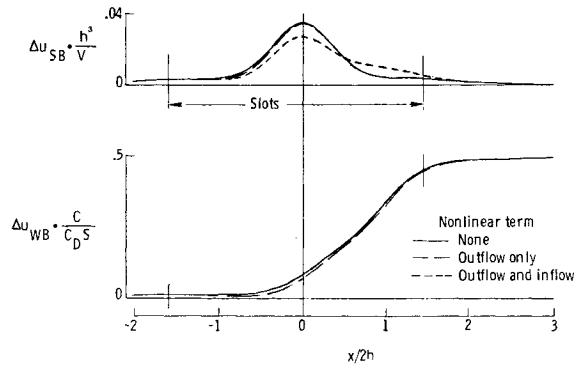

a) Solid blockage and wake blockage cases.

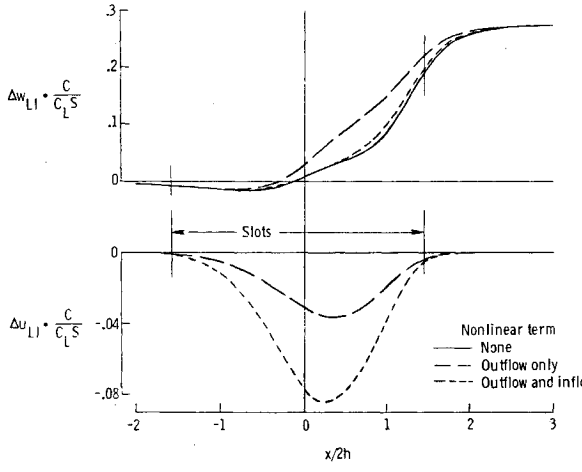

b) Lift interference case.

Fig. 9 Effects of nonlinear slot boundary condition on wall-induced velocities on tunnel axis.

solid blockage, $C_D{}^{S/C} = .02$ for wake blockage, and $C_L{}^{S/C} = .04$ for lift interference.

The solid blockage and wake blockage results given on Fig. 9a show that only minor changes in wall interference result from the outflow dynamic pressure effect. The solid blockage results, however, are affected significantly by the nonlinear inflow feature.

In the case of lift interference, shown on Fig. 9b, both the magnitude and gradient of the wall-induced upwash at the model are increased by the outflow dynamic pressure effect, but this change is essentially canceled by including the inflow nonlinearity. It is apparent that the outflow dynamic pressure effect increases the constraint against outflow, causing the bottom wall to act more like a solid wall; whereas the inflow nonlinearity reduces the constraint against inflow, causing the top wall to act more like an open jet boundary.

The most important effect of the nonlinearities, however, is to cause a decrement in longitudinal velocity as part of the wall interference due to lift. Both the outflow through the bottom wall and the inflow through the top wall reach their largest magnitudes downstream of the model. Both types of nonlinearity contribute to an excess of inflow over outflow in this region. Maintenance of mass balance in the plenum requires a reduction in plenum pressure which, in turn, causes outflow through the slots upstream of the model on both the top and bottom walls. A part of the tunnel flow is thereby diverted out of the test section, causing a reduction in longitudinal velocity at the model. For the case shown in Fig. 9, the magnitude of this velocity decrease is much greater than the velocity increase due to solid blockage.

It should be noted that a detailed examination of the performance of the nonlinear slot inflow model has shown that the desired boundary condition at the surface of the slot inflow bubble is met only approximately. The error observed is generally in the direction to cause some overprediction of the nonlinear effects of slot inflow.

Concluding Remarks

A numerical model of a slotted wind tunnel test has been developed to be used with sparsely measured wall pressures for wall interference assessment. By using the model as a wall interference prediction tool, it is demonstrated that accounting for slot discreteness is important in interpreting wall pressures measured between slots, and that accounting for finite slot length and nonlinear effects in a slot boundary condition can yield significant departures from the wall interference predicted using the classical linear homogeneous infinite length wall representation. In particular, a significant cross coupling between model lift and the longitudinal interference velocity results from use of the nonlinear slot boundary conditions.

Acknowledgment

The support of NASA Langley Research Center under Cooperative Agreement NCC1-69 for the work reported herein is gratefully acknowledged.

References

[1]Kemp, W. B. Jr. and Adcock, J. B., "Combined Four-Wall Interference Assessment in Two-Dimensional Airfoil Tests," *AIAA Journal*, Vol. 21, Oct. 1983, pp. 1353-1359.

[2]Mokry, M. and Ohman, L. H., "Application of the Fast Fourier Transform to Two-Dimensional Wind Tunnel Wall Interference," *Journal of Aircraft*, Vol. 17, June 1980, pp. 402-408.

[3]Mokry, M., Chan, Y. Y., and Jones D. S., "Two-Dimensional Wind Tunnel Wall Interference," AGARDograph No. 281, Nov. 1983.

[4]Mokry, M., "Subsonic Wall Interference Corrections for Finite-Length Test Sections using Boundary Pressure Measurements," AGARD CP 335, Paper 10, May 1982.

[5]Rizk, M. H., and Smithmeyer, M. G., "Wind Tunnel Wall Interference Corrections for Three-Dimensional Flows," *Journal of Aircraft*, Vol. 19, June 1982, pp. 465-472.

[6]Rizk, M. H., and Murman, E. M., "Wind Tunnel Wall Interference Corrections for Aircraft Models in the Transonic Regime," *Journal of Aircraft*, Vol. 21, Jan. 1984, pp. 54-61.

[7]Sedin, Y. C-J and Sorensen, H., "Computed and Measured Wall Interference in a Slotted Transonic Test Section," AIAA Paper 84-0243, Jan. 1984.

[8]Thomas, J. L., Luckring, J. M., and Sellers, W. L., III, "Evaluation of Factors Determining the Accuracy of Linearized Subsonic Panel Methods," AIAA Paper 83-1826, July 1983.

[9]Berndt, S. B., "Inviscid Theory of Wall Interference in Slotted Test Sections," *AIAA Journal*, Vol. 15, Sept. 1977, pp. 1278-1287.

[10]Steinle, F. W. Jr. and Pejack, E. R., "Toward an Improved Transonic Wind-Tunnel-Wall Geometry—A Numerical Study," AIAA Paper 80-0442, March 1980.

[11]Lo, C. F. and Glassman, H. N., "Calculation of Interference for a Porous Wall Wind Tunnel by the Method of Block Cyclic Reduction," AEDC-TR-75-98, Nov. 1975.

[12]Slooff, J. W. and Piers, W. J., "The Effect of Finite Test Section Length on Wall Interference in 2-D Ventilated Windtunnels," *Windtunnel Design and Testing Techniques*, AGARD CP 174, Oct. 1975, Paper 14, 11 pp.

[13]Wood, W. W., "Tunnel Interference from Slotted Walls," *Quarterly Journal of Mechanics and Applied Mathematics*, Vol. 17, May 1964, pp. 126-140.

[14]Berndt, S. B. and Sorensen, H., "Flow Properties of Slotted Walls for Transonic Test Sections," AGARD CP 174, Paper 17, Oct. 1975.

[15]Davis, D. D. Jr. and Moore, D., "Analytical Studies of Blockage- and Lift-Interference Corrections for Slotted Tunnels Obtained by the Substitution of an Equivalent Homogeneous Boundary for the Discrete Slots," NACA RM-L53E07b, June 1953.

[16]Pindzola, M. and Lo, C. F., "Boundary Interference at Subsonic Speeds in Wind Tunnels with Ventilated Walls," AEDC TR-69-47, May 1969.

[17]Barnwell, R. W., "Design and Performance Evaluation of Slotted Walls for Two-Dimensional Wind Tunnels," NASA TM X-78648, Feb. 1978.